THE JOURNAL OF BIOLOGICAL CHEMISTRY VOL. 287, NO. 13, pp. 9862–9872, March 23, 2012

cAMP Induces Stromal Interaction Molecule 1 (STIM1) Puncta but neither Orai1 Protein Clustering nor Store-operated Ca^{2+} Entry (SOCE) in Islet Cells*

Received for publication, August 11, 2011, and in revised form, January 30, 2012 Published, JBC Papers in Press, February 1, 2012, DOI 10.1074/jbc.M111.292854

Geng Tian[‡], Alexei V. Tepikin[§], Anders Tengholm[‡], and Erik Gylfe[‡1]

From the [‡]Department of Medical Cell Biology, Uppsala University, BMC Box 571, SE-751 23 Uppsala, Sweden and the [§]Physiological Laboratory, Department of Cellular and Molecular Physiology, University of Liverpool, Liverpool L69 3BX, United Kingdom

Background: Regulation of the ER Ca^{2+} sensor STIM1 and its association with the plasma membrane channel Orai1 to activate store-operated Ca^{2+} entry (SOCE) remains incompletely understood.
Results: cAMP induced plasma membrane translocation of STIM1 in islet cells without concomitant SOCE activation.
Conclusion: STIM1 translocation alone is insufficient to activate SOCE.
Significance: This study describes novel interaction between the components of cAMP and Ca^{2+} signaling cascades.

The events leading to the activation of store-operated Ca^{2+} entry (SOCE) involve Ca^{2+} depletion of the endoplasmic reticulum (ER) resulting in translocation of the transmembrane Ca^{2+} sensor protein, stromal interaction molecule 1 (STIM1), to the junctions between ER and the plasma membrane where it binds to the Ca^{2+} channel protein Orai1 to activate Ca^{2+} influx. Using confocal and total internal reflection fluorescence microscopy, we studied redistribution kinetics of fluorescence-tagged STIM1 and Orai1 as well as SOCE in insulin-releasing β-cells and glucagon-secreting α-cells within intact mouse and human pancreatic islets. ER Ca^{2+} depletion triggered accumulation of STIM1 puncta in the subplasmalemmal ER where they co-clustered with Orai1 in the plasma membrane and activated SOCE. Glucose, which promotes Ca^{2+} store filling and inhibits SOCE, stimulated retranslocation of STIM1 to the bulk ER. This effect was evident at much lower glucose concentrations in α- than in β-cells consistent with involvement of SOCE in the regulation of glucagon secretion. Epinephrine stimulated subplasmalemmal translocation of STIM1 in α-cells and retranslocation in β-cells involving raising and lowering of cAMP, respectively. The cAMP effect was mediated both by protein kinase A and exchange protein directly activated by cAMP. However, the cAMP-induced STIM1 puncta did not co-cluster with Orai1, and there was no activation of SOCE. STIM1 translocation can consequently occur independently of Orai1 clustering and SOCE.

Based on studies in nonexcitable cells, Putney (1) proposed the existence of a store-operated or capacitative pathway for Ca^{2+} entry into cells. The store-operated Ca^{2+} entry (SOCE)[2] through the plasma membrane (PM) is activated by release of Ca^{2+} from the endoplasmic reticulum (ER) in response to Ca^{2+}-mobilizing messengers like inositol 1,4,5-trisphosphate (IP_3). Some of the released Ca^{2+} is inevitably transported out of the cell, and the SOCE compensates for this loss and ensures proper Ca^{2+} refilling of the ER. The molecular mechanisms underlying the SOCE remained elusive for almost 2 decades until it was discovered that the stromal interacting molecule 1 (STIM1) has a role in store-operated entry (2, 3). STIM1 and the structurally related STIM2 are single pass transmembrane molecules in the ER, and STIM proteins are also present in the PM (4). Both molecules contain Ca^{2+}-sensing EF-hand motifs in their N termini facing the ER lumen and are believed to sense the Ca^{2+} depletion that activates SOCE (3, 5, 6). Another molecule in the PM named Orai was identified as an important player in the store-operated mechanism (7–9). There are three isoforms of Orai (Orai1–3), and evidence has accumulated that Orai is the pore-forming unit of the store-operated channel (10–14). Emptying of Ca^{2+} from the ER results in dissociation of the ion from STIM1, which rapidly moves and aggregates in the subplasmalemmal ER where it forms distinct puncta (3, 12, 15, 16), and this is the site where STIM interacts with Orai to activate SOCE (11, 17, 18).

The store-operated pathway is also present in excitable cells like the insulin-releasing β- and glucagon-secreting α-cells. Although these cells have more potent voltage-operated routes for Ca^{2+} entry, SOCE has been found to be important for different cellular processes. However, even maximally activated SOCE has modest effects on the cytoplasmic Ca^{2+} concentration ($[Ca^{2+}]_i$) in β- (19–21) and α-cells (22) and has mostly been attributed a functional role based on the depolarizing effect (22–24). Whereas Ca^{2+} depletion of the ER has little effect on the membrane potential (20) and insulin release (24)

* This work was supported by grants from the Swedish Research Council, the Swedish Diabetes Association, NovoNordisk Foundation, European Foundation for the Study of Diabetes and Merck Sharp and Dohme (EFSD/MSD), and the Family Ernfors Foundation.
[1] To whom correspondence should be addressed. Tel.: 46-18-471-4428; Fax: 46-18-471-4059; E-mail: erik.gylfe@mcb.uu.se.
[2] The abbreviations used are: SOCE, store-operated Ca^{2+} entry; PM, plasma membrane; ER, endoplasmic reticulum; IP_3, inositol 1,4,5-trisphosphate; Epac, exchange protein directly activated by cAMP; CFP, cyan fluorescent protein; DDA, 2′5′-dideoxyadenosine; CPA, cyclopiazonic acid; IBMX, 3-isobutyl-1-methylxanthine; VOCC, voltage-operated Ca^{2+} channel; SERCA, sarcoendoplasmic reticulum Ca^{2+}-ATPase; ROI, region of interest; TIRF, total internal reflection fluorescence.

from β-cells exposed to a sub-stimulatory glucose concentration (3 mM), such depletion further depolarizes glucose-stimulated β-cells (23) and amplifies insulin secretion (23, 24). Activation of SOCE has much more important effects on the α-cell by triggering Ca^{2+} entry through voltage-operated Ca^{2+} channels (VOCCs) (22) and glucagon release (24), and SOCE has been attributed to be a central function in epinephrine stimulation and glucose inhibition of glucagon secretion (22, 24).

Studies of the store-operated mechanism in primary β-cells (21, 25) and α-cells (22) have been based on measurements of $[Ca^{2+}]_i$ in Ca^{2+} omission-readdition (21, 22, 25) and Mn^{2+} quench (21, 25) experiments. Direct studies of molecules involved in the store-operated mechanism have so far been restricted to clonal MIN6 β-cells transfected with STIM1 tagged with enhanced yellow fluorescent protein (STIM1-YFP) showing that Ca^{2+} depletion of the ER triggers the expected PM association of the molecule (26). We have now utilized adenoviruses encoding STIM1-YFP and Orai1-mCherry (16) to infect pancreatic islets and study STIM1 translocation and association with Orai1 in primary pancreatic islet cells during conditions known to modulate hormone secretion and SOCE. Consistent with a role of SOCE in glucagon secretion, the Ca^{2+} entry was controlled by similar low glucose concentrations in α-cells as those regulating release of the glucose-elevating hormone. We also discovered that cAMP triggers STIM1 translocation to the subplasmalemmal regions but neither induces co-clustering of STIM1-Orai1 nor the activation of SOCE that occurs after calcium depletion of the ER. The data indicate that STIM1 translocation can occur independent of Orai1 clustering and SOCE.

EXPERIMENTAL PROCEDURES

Chemicals—Epinephrine, cyclopiazonic acid (CPA), 2′5′-dideoxyadenosine (DDA), 3-isobutyl-1-methylxanthine (IBMX), carbachol, forskolin, poly-L-lysine, EGTA, HEPES, and methoxyverapamil were purchased from Sigma, and RPMI 1640 medium and fetal bovine serum were from Invitrogen. Biolog Life Science Institute (Bremen, Germany) supplied N^6-phenyladenosine-3′,5′-cyclic monophosphate, 8-(4-chlorophenyl-thio)adenosine-3′,5′-cyclic monophosphorothioate, S_p isomer (S_p-8-CPT-cAMPS), and 8-(4-chlorophenylthio)-2′-*O*-methyladenosine-3′,5′-cyclic monophosphate, acetoxymethyl ester. The acetoxymethyl ester of the Ca^{2+} indicator Fura-PE3 was obtained from TEFLabs (Austin, TX). Tris was from Merck; diazoxide was from Schering-Plough (Rathdrum, Ireland); and serum-free protein block, rabbit anti-glucagon and guinea pig anti-insulin were bought from DAKO (Glostrup, Denmark). The MACH 3™ rabbit probe alkaline phosphate polymer kit was from Biocare (Concord, CA). Mayer's hematoxylin was bought from HistoLab (Gothenburg, Sweden). Adenoviruses expressing STIM1-YFP and Orai1-mCherry were produced as described previously (16).

Islet Isolation, Cell Culture, and Virus Infection—All procedures for animal handling, preparation, and use of pancreatic islets were approved by local animal and human ethical committees. Islets of Langerhans were isolated from C57BL6J female mice. The animals were placed in a sealed container into which a stream of CO_2 was delivered. When the animals became unconscious, they were exsanguinated by decapitation. After opening the peritoneal cavity, the splenic part of the pancreas was excised and cut into small pieces, which were digested with 1 mg/ml collagenase to obtain free islets of Langerhans. Human pancreatic islets from five normoglycemic cadaveric donors (two female, three male; aged 39–57 years) were generously provided by the Nordic Network for Clinical Islet Transplantation. The islets were isolated with semiautomated digestion filtration (27) and purified on a continuous density gradient in a refrigerated cell processor (COBE 2191; COBE Blood Component Technology, Lakewood, CO). After purification, the islets were kept for 2–5 days at 37 °C in an atmosphere of 5% CO_2 in CMRL 1066 culture medium (Mediatech, Herndon, VA) containing 5.5 mM glucose and supplemented with 10 mM nicotinamide, 10 mM HEPES, 0.25 μg/ml Fungizone, 50 μg/ml gentamicin, 2 mM glutamine, 10 μg/ml ciprofloxacin, and 10% fetal calf serum. The islets were subsequently cultured for 1–4 days in RPMI 1640 medium containing 5.5 mM glucose and supplemented with 10% fetal calf serum, 100 μg/ml penicillin, and 100 μg/ml streptomycin. The islets were then infected with adenovirus encoding STIM1-YFP and/or Orai1-mCherry using a multiplicity of infection of 10^5 fluorescent focus-forming units/islet in culture medium. After 1 h of incubation at 37 °C, the inoculum was removed, and the islets were washed twice, followed by further culture for 24 h. To check that fluorescence changes did not merely reflect alterations of membrane properties and/or cell adhesion, some measurements were performed after co-infection with adenovirus encoding cyan fluorescent protein (CFP) anchored to the PM as reference (28). Before the experiments, the islets were transferred to a buffer containing 125 mM NaCl, 4.8 mM KCl, 1.3 mM $CaCl_2$, 1.2 mM $MgCl_2$, and 25 mM HEPES (with pH adjusted to 7.40 with NaOH) and incubated for 30 min at 37 °C. The islets were then allowed to attach to the center of polylysine-coated round 25-mm coverslips for 5 min. Some experiments were performed on single cells prepared by shaking the freshly isolated islets in a Ca^{2+}-deficient medium (29). After resuspension in the RPMI 1640 culture medium, the cells were allowed to attach to the center of round coverslips during 2–5 days of culture at 37 °C in an atmosphere of 5% CO_2 in humidified air.

Measurements of STIM1-YFP Translocation and Redistribution of Orai1-mCherry—The subcellular distribution of the STIM1-YFP fluorescence was analyzed with a Yokogawa CSU-10 spinning disk confocal system (Andor Technology, Belfast, Northern Ireland) attached to a TE2000 microscope (Nikon) with a ×60 1.40 NA objective (Nikon). The fluorescence was excited by the 514-nm line of an argon ion laser (ALC ×60, Creative Laser Corp, Munich, Germany). The laser beam was homogenized and expanded by a rotating light-shaping diffuser (Physical Optics Corp., Torrance, CA) before being refocused into the confocal scanhead. Fluorescence emission was selected by a 560-/40-nm half-bandwidth filter (Semrock, Rochester, NY) and detected with a back-illuminated EMCCD camera (DU-888, Andor Technology) under MetaFluor (Molecular Devices Corp., Downington, PA) software control. An Eclipse Ti microscope (Nikon) with a total internal reflection fluorescence (TIRF) illuminator and a ×60 1.45 NA objective was used for measurements of the PM concentrations of

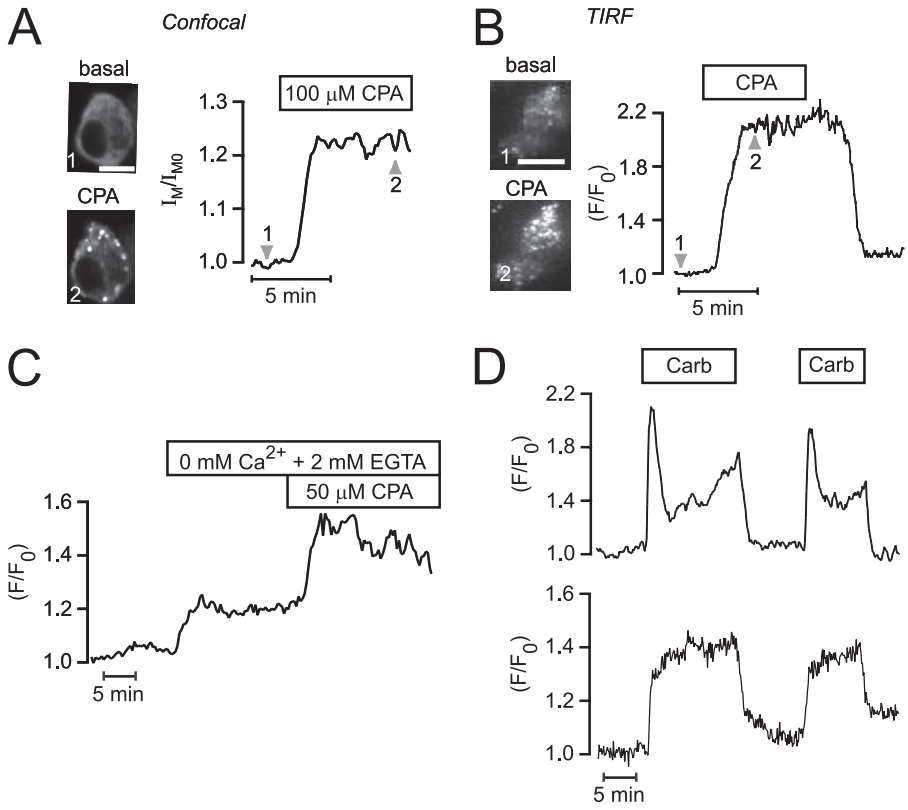

FIGURE 1. **STIM1-YFP translocation and subplasmalemmal puncta formation after Ca^{2+} store depletion in pancreatic islet cells.** *A*, confocal images showing STIM1-YFP translocation and subplasmalemmal puncta formation in response to Ca^{2+} depletion of the ER with 100 μM of the SERCA inhibitor CPA in a superficial islet cell. The *trace* shows changes in PM-adjacent fluorescence with time, and the *numbered arrowheads* indicate when respective images were taken. *B*, TIRF images showing STIM1-YFP translocation and subplasmalemmal puncta formation in response to Ca^{2+} depletion of the ER with 100 μM of the SERCA inhibitor CPA in a superficial islet cell. The *trace* shows changes in average TIRF intensity with time, and the *numbered arrowheads* indicate when respective images were taken. *C*, TIRF intensity recording showing subplasmalemmal accumulation STIM1-YFP in Ca^{2+}-deficient medium (0 mM Ca^{2+} and 2 mM EGTA) and during subsequent exposure to 50 μM CPA in a superficial islet cell. *D*, TIRF intensity recordings showing different patterns of carbachol (*Carb*)-induced (50 μM) subplasmalemmal accumulation of STIM1-YFP. The glucose concentration was 3 mM in all panels.

STIM1-YFP, CFP-tagged PM marker, and Orai1-mCherry. The 514- and 458-nm lines of an argon laser (Creative Laser Production) were used for excitation of YFP and CFP, respectively, and the 561-nm line of a diode-pumped solid-state laser (Jive, Cobolt AB, Stockholm, Sweden) was used to excite mCherry. However, because of the properties of the dichroic mirror, the 488-nm line of the argon laser was used to excite YFP when measured in parallel with mCherry. Wavelengths were selected by interference filters (Semrock) mounted in a filter wheel (Sutter Instruments, Novato, CA), and the beam was coupled to the TIRF illuminator by an optical fiber (Oz Optics, Ottawa, Canada). Fluorescence was detected with a back-illuminated EMCCD camera (DU-887, Andor Technology) controlled by the MetaFluor software. Emission wavelengths were selected with interference filters (560-/40-nm half-bandwidth for YFP, 485-/25-nm for CFP; Semrock) or a glass filter (645-nm long pass for mCherry; Melles Griot) mounted in a filter wheel (Sutter Instruments). YFP or mCherry images and YFP/CFP or YFP/mCherry image pairs were acquired every 5 s. The beam was blocked by a shutter (Sutter Instruments) between image captures to minimize exposure of the cells to the potentially harmful laser light. The coverslips with the attached islets were used as exchangeable bottoms of an open custom-built 50-μl laminar flow chamber. The chamber holder on the microscope stage and the objective were thermostated at 37 °C. Islets in the chamber were superfused with medium at a rate of 0.3 ml/min.

Measurements of $[Ca^{2+}]_i$—For $[Ca^{2+}]_i$ measurements, the cells were preincubated in the presence of 1 μM of the acetoxymethyl ester of Fura-PE3. $[Ca^{2+}]_i$ imaging was performed with an inverted microscope (Nikon Diaphot) placed in a climate box maintained at 37 °C. The microscope was equipped for epifluorescence fluorometry with a 400-nm dichroic mirror and a ×40 1.3 NA Fluor oil immersion objective. Excitation light was delivered through a 5-mm diameter liquid light guide from an Optoscan monochromator (Cairn Research Ltd., Faversham, UK) with a 150-watt xenon arc lamp. The monochromator provided excitation light at 340 nm (2.5-nm half-bandwidth) and 380 nm (1.9-nm half-bandwidth), and emission was measured at 510 nm (40-nm half-bandwidth) using a EMCCD camera (DU-887, Andor Technology). The Metafluor software controlled the monochromator and the camera, acquiring image pairs every 2 s with 80–100-ms integration at each wavelength and <1 ms for changing wavelength and slits. To reduce photodamage, the specimens were illuminated only during image capture. Ratio frames were calculated after background subtraction, and $[Ca^{2+}]_i$ was estimated as described previously (30).

Cell Identification—Immediately after experiments, α- and β-cells remaining in position within the experimental chamber in the microscope were identified by immunostaining for glucagon and insulin. The cells were fixed by sequential 5-min exposures to 25, 50, 75, and 95% ethanol. After sequential rinsing with 3% H_2O_2 and Tris buffer (0.05 M, pH 7.4), protein block was added to reduce background staining. After 10 min, polyclonal rabbit anti-glucagon or guinea pig anti-swine insulin (1:100; DAKO) was added for 30 min followed by rinsing with Tris buffer. The MACH 3™ rabbit probe alkaline phosphatase polymer kit was then used for the visualization according to manufacturer's instructions. After further rinsing with Tris buffer and distilled water, cell nuclei were stained with hematoxylin for 0.5–2 min. The α-cells are smaller than the β-cells, and the two cell types show opposite responses to epinephrine with regard to STIM1-YFP translocation between the bulk ER and the subplasmalemmal junctions (see "Results"). Therefore, the size of the cell footprint together with the translocation response to epinephrine was used for cell identification in most experiments. These criteria should eliminate the small somatostatin-releasing δ-cells with β-cell-like domination of α_2-adrenoceptors (31) as small cells and cells with small footprints were never taken as β-cells. Because epinephrine mobilizes intracellular Ca^{2+} in α- but not β-cells (22), this response together with cell size was used for cell identification in most measurements of $[Ca^{2+}]_i$.

Data and Statistical Analysis—Image analysis was made using the MetaFluor or ImageJ (W. S. Rasband, National Institutes of Health, rsb.info.nih.gov) software. The STIM1-YFP concentration in the subplasmalemmal region was evaluated as the fluorescence intensity F in relation to the initial fluorescence intensity F_0 after subtraction of background (F/F_0). To quantify the redistribution of Orai1 in the PM, we analyzed the intensity variability in the Orai1 images by calculating the variation coefficient of pixel intensities. The pixel size was 266 nm, which is close to the theoretical 222-nm optical resolution in 645 nm of light. Data are presented as means ± S.E. Statistical comparisons were assessed with Student's t test.

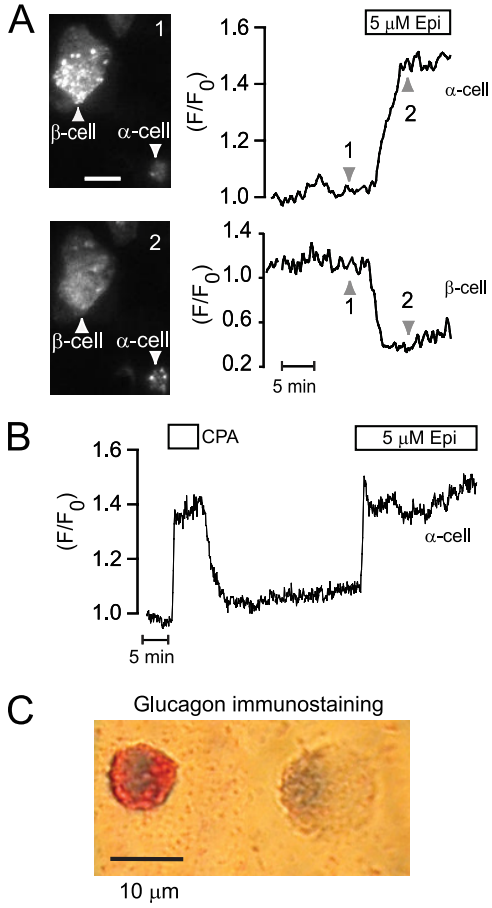

FIGURE 2. **Epinephrine triggers opposite translocation of STIM1-YFP in pancreatic α- and β-cells.** *A*, TIRF images and intensity recordings showing accumulation of the subplasmalemmal STIM1-YFP in response to 5 μM epinephrine (*Epi*) in a superficial islet cell with a small footprint (α-cell) and the loss of subplasmalemmal STIM1-YFP in an adjacent cell with larger footprint (β-cell) within an islet. The *numbered arrowheads* indicate when respective images were taken. *B*, TIRF intensity recording of a superficial islet cell (α-cell) responding to 100 μM CPA and 5 μM epinephrine with subplasmalemmal accumulation of STIM1-YFP. *C*, immunostaining showing that a small islet cell responding to epinephrine with subplasmalemmal accumulation of STIM1-YFP is a glucagon-positive α-cell (*left*). Staining for insulin showed that the larger cells with opposite responses to epinephrine are β-cells (data not shown). The glucose concentration was 3 mM in all panels and the image *scale bars* indicate 10 μm.

RESULTS

Depletion of ER Ca^{2+} Induces Subplasmalemmal STIM1 Accumulation—Peripheral cells in isolated mouse islets expressing STIM1-YFP and exposed to 3 mM glucose showed diffuse fluorescence over the cytoplasm in confocal microscopy (Fig. 1*A*), but also some subplasmalemmal fluorescence puncta were observed with TIRF microscopy (Fig. 1*B*). Depletion of the ER Ca^{2+} stores by inhibition of the sarcoendoplasmic reticulum Ca^{2+}-ATPase (SERCA) with CPA induces gradual formation of much more conspicuous subplasmalemmal puncta (52 ± 4-s rise time; Fig. 1, *A* and *B*). This CPA effect was delayed 118 ± 21 s (n = 13). Omission of extracellular Ca^{2+} with addition of EGTA induced a less marked subplasmalemmal accumulation of STIM1-YFP that was further enhanced by CPA (Fig. 1*C*).

The cholinergic agonist carbachol (50 μM), which raises IP_3 and mobilizes ER Ca^{2+} both in α-cells (22) and β-cells (19), induced sustained subplasmalemmal accumulation of STIM1-YFP preceded (3 of 8) or not by an initial peak in most islet cells exposed to 3 mM glucose (Fig. 1*D*). Both the delay before the onset of STIM1 translocation (28 ± 4 s; n = 8) and the rise time (22 ± 4 s) were much shorter than after CPA exposure (4- and 2.4-fold difference, respectively, $p < 0.001$).

Epinephrine Induces Opposite Translocation of STIM1 in α- and β-Cells—In the presence of 3 mM glucose, the addition of 5 μM epinephrine induced opposite responses in different cells. In the majority of the cells (27 of 41), TIRF microscopy revealed epinephrine-induced loss of PM-associated STIM1-YFP fluorescence indicating retranslocation of the protein from the subplasmalemmal region into the bulk ER (Fig. 2*A*). In 5 of the 41 cells that had smaller footprints, epinephrine instead induced pronounced subplasmalemmal accumulation of STIM1-YFP with formation of distinct puncta. Fig. 2*B* shows that one of the latter cells also responded to CPA with similar STIM1-YFP translocation to the PM. There was no epinephrine response in the remaining nine cells (data not shown). Immunostaining for

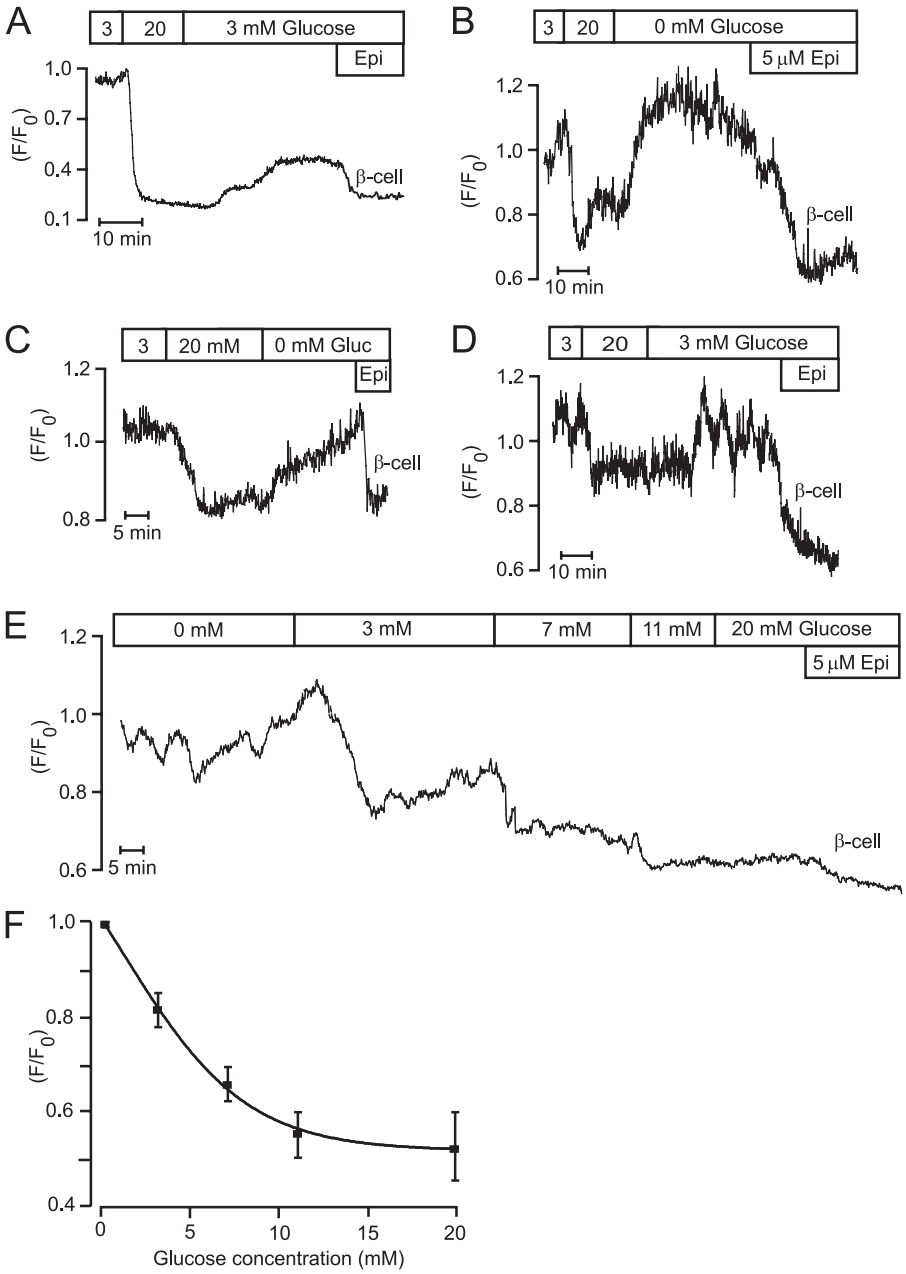

FIGURE 3. **Glucose reduces subplasmalemmal STIM1-YFP fluorescence in islet β-cells.** *A–C,* TIRF intensity recordings on epinephrine-identified β-cells (*Epi,* 5 μM) showing that increase of the glucose concentration from 3 to 20 mM reduces subplasmalemmal STIM1-YFP fluorescence. The glucose effect was partially reversed after reintroduction of 3 mM glucose (*A*) and complete reversal required glucose omission in islet β-cells (*B* and *C*). *D,* TIRF intensity recording of a β-cell with STIM1-YFP oscillations in 3 mM glucose (*Gluc*) that are reversibly inhibited by 20 mM glucose. *E,* TIRF intensity recording of the effect of increasing glucose concentrations within the 0–20 mM range on reduction of subplasmalemmal STIM1-YFP in a single β-cell. *F,* dose-response relationships for glucose-induced reduction of subplasmalemmal STIM1-YFP in β-cells. Mean values ± S.E., $n = 9$.

insulin and glucagon revealed that the epinephrine-induced decrease and increase of subplasmalemmal STIM1-YFP occurred in β-cells (data not shown) and α-cells (Fig. 2*C*), respectively.

Glucose Stimulates Retranslocation of STIM1 to Bulk ER—Increase of the glucose concentration from 3 to 20 mM resulted in loss of subplasmalemmal STIM1-YFP fluorescence in β-cells identified by size and epinephrine response (21 of 32; Fig. 3). In most cases, this glucose effect was only partially reversed after reintroduction of 3 mM glucose (Fig. 3*A*), and rapid restoration of subplasmalemmal STIM1-YFP fluorescence required glucose omission (Fig. 3, *B* and *C*). Some β-cells (19 of 167) showed oscillations of subplasmalemmal STIM1-YFP fluorescence in 3 mM glucose that were reversibly inhibited by 20 mM of the sugar (all of five β-cells; Fig. 3*D*). Fig. 3*E* exemplifies the glucose concentration dependence of the loss of subplasmalemmal STIM1-YFP fluorescence, and Fig. 3*F* summarizes similar observations in nine β-cells with half-maximal and maximal effects at 3.4 and 11 mM, respectively.

Also size- and epinephrine-identified α-cells responded to glucose with reduction of PM-associated STIM1-YFP fluorescence (Fig. 4*A*). Because this effect was maximal when glucose had been increased from 0 to 3 mM, we tested additional concentrations within this range. Fig. 4, *B* and *C,* shows two α-cells

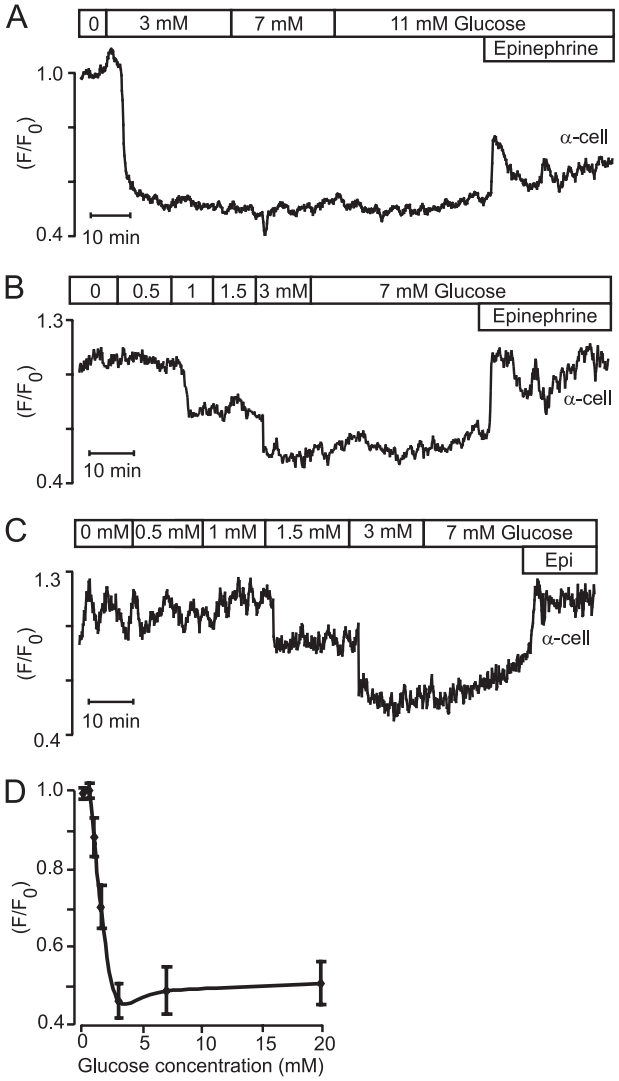

FIGURE 4. **Glucose reduction of subplasmalemmal STIM1-YFP fluorescence in islet α-cells is maximal already at 3 mM.** *A–C*, TIRF intensity recordings on epinephrine-identified (5 μM) α-cells showing that 3 mM glucose is sufficient for maximal reduction of subplasmalemmal STIM1-YFP fluorescence. Some α-cells showed STIM1-YFP oscillations in the absence of glucose (*C*). *D*, dose-response relationships for glucose-induced reduction of subplasmalemmal STIM1-YFP in α-cells. Mean values ± S.E., $n = 5$.

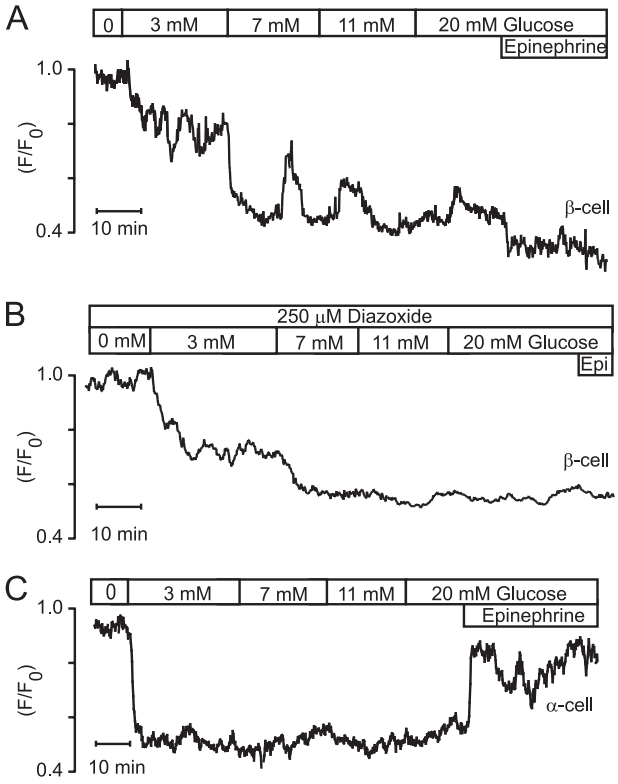

FIGURE 5. **Glucose-induced reduction of subplasmalemmal STIM1-YFP fluorescence in human β- and α-cells.** *A*, TIRF intensity recording of an epinephrine-identified (5 μM) β-cell showing that the glucose-induced reduction of subplasmalemmal STIM1-YFP fluorescence is interrupted by peaks of STIM1-YFP increase. *B*, monotonous reduction of subplasmalemmal STIM1-YFP fluorescence by increasing glucose concentrations after hyperpolarization of an epinephrine-identified (*Epi*, 5 μM) β-cell with diazoxide. *C*, reduction of subplasmalemmal STIM1-YFP fluorescence in an epinephrine-identified (5 μM) α-cell is maximal already at 3 mM glucose.

starting to respond to reduction of PM-associated STIM1-YFP fluorescence at 1 and 1.5 mM glucose, respectively, and Fig. 4*D* summarizes the concentration dependence with half-maximal and maximal effects at 1.3 and 3 mM. Some α-cells showed oscillations in subplasmalemmal STIM1-YFP fluorescence in glucose-free medium (6 of 21; Fig. 4*C*), and these oscillations were inhibited by glucose. The epinephrine response was not always sustained like in the α-cells shown in Figs. 2, *A* and *B*, and 4, *B* and *C*. In 7 of 51 α-cells, the response was instead transient (Figs. 4*A*, and 6*B*).

The glucose-induced STIM1-YFP retranslocation from the subplasmalemmal region to the bulk ER was also studied in human pancreatic islets. Fig. 5, *A* and *B*, shows traces obtained with epinephrine-identified β-cells and that in Fig. 5*C* from an α-cell. Like in mouse β-cells, glucose induced concentration-dependent translocation, but at ≥7 mM the gradual reduction of subplasmalemmal fluorescence was interrupted by peaks of PM fluorescence in all five β-cells (Fig. 5*A*). This phenomenon may reflect activation of the store-operated pathway by Ca^{2+}-induced Ca^{2+} release from the ER triggered by Ca^{2+} entry through VOCCs. We therefore repeated experiments under conditions preventing such entry. As shown in Fig. 5*B*, increasing glucose concentrations monotonously reduced subplasmalemmal STIM1-YFP fluorescence in the presence of the hyperpolarizing ATP-sensitive K^+ (K_{ATP}) channel activator diazoxide with maximal effect at 7–11 mM of the sugar in two studied β-cells. Also, four human α-cells behaved similarly to mouse α-cells with maximal loss of subplasmalemmal fluorescence already with 3 mM glucose (Fig. 5*C*).

cAMP Induces Subplasmalemmal STIM1 Accumulation Involving PKA and Epac—Because epinephrine acts on α_1- (32) and β-adrenoceptors (32, 33) in α-cells to increase IP_3 and cAMP (34) resulting in Ca^{2+} release from the ER, it was not surprising that epinephrine induced subplasmalemmal accumulation of STIM1-YFP. However, the opposite effect in β-cells was unexpected considering that epinephrine acts on α_2-adrenoceptors (33, 35) to lower cAMP (34). We therefore tested whether changes in cAMP might be involved in the STIM1 translocation responses of the two cell types. These experiments were done at a basal glucose concentration to prevent cAMP from promoting IP_3 receptor-mediated Ca^{2+} release, which only occurs in β-cells exposed to higher concen-

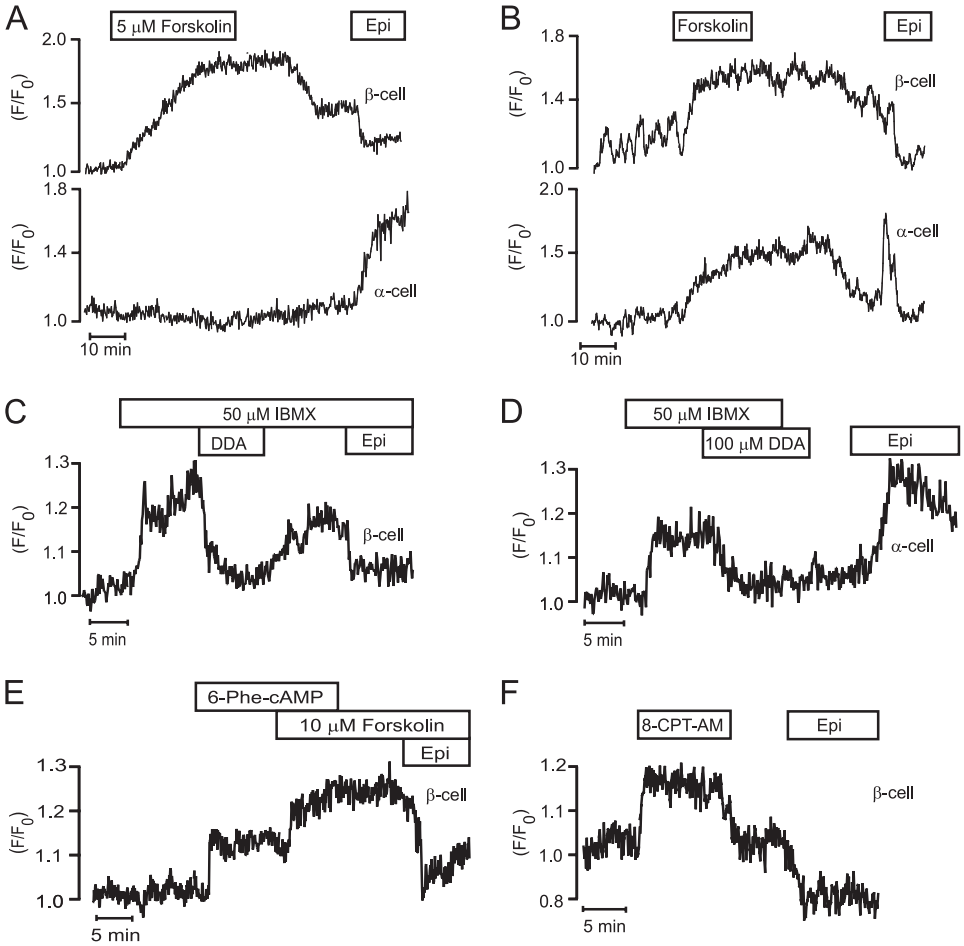

FIGURE 6. **cAMP induces subplasmalemmal accumulation of STIM1-YFP.** TIRF intensity recordings of subplasmalemmal fluorescence of STIM1-YFP in cells within pancreatic islets. *A* and *B*, adenylyl cyclase activator forskolin (5 μM) increases subplasmalemmal fluorescence of STIM1-YFP in epinephrine-identified (*Epi*, 5 μM) α- and β-cells. *C*, phosphodiesterase inhibitor IBMX (50 μM) increases subplasmalemmal STIM1-YFP fluorescence, and the adenylyl cyclase inhibitor DDA (100 μM) reverses this effect in an epinephrine-identified (5 μM) β-cells. *D*, IBMX increases subplasmalemmal STIM1-YFP fluorescence, and DDA reverses this effect in an epinephrine-identified (5 μM) α-cells. *E*, specific PKA agonist N^6-phenyladenosine-3′,5′-cyclic monophosphate (*6-Phe-cAMP*) (100 μM) increases subplasmalemmal STIM1-YFP fluorescence and forskolin (10 μM) has additional effect in an epinephrine-identified (5 μM) β-cell. *F*, specific Epac agonist 8-(4-chlorophenylthio)-2′-*O*-methyladenosine-3′,5′-cyclic monophosphate, acetoxymethyl ester (*8-CPT-AM*) (1 μM) increases subplasmalemmal STIM1-YFP fluorescence in an epinephrine-identified (5 μM) β-cell. The glucose concentration was 3 mM in all panels.

trations of the sugar (36, 37). Because $[Ca^{2+}]_i$ in β-cells is low and stable under these conditions, the reported effects of $[Ca^{2+}]_i$ elevation on STIM1 translocation (38) should not influence the results. Fig. 6, *A* and *B*, shows that the rise of cAMP by activation of adenylyl cyclases with 5 μM forskolin increased STIM1-YFP translocation to the PM in 22 of 27 β-cells with opposite response to epinephrine. Also, most epinephrine-identified α-cells (6 of 8) reacted to forskolin in a similar manner (Fig. 6*B*), and the remaining α-cells did not respond (Fig. 6*A*). Fig. 6, *C* and *D*, illustrates that STIM1-YFP translocation to the PM after rise of cAMP by phosphodiesterase inhibition with 50 μM IBMX is reversed by 100 μM of the adenylyl cyclase inhibitor DDA in all of 10 β-cells (Fig. 6*C*) and all of 9 α-cells (Fig. 6*D*) identified with epinephrine. Also, the specific PKA agonists N^6-phenyladenosine-3′,5′-cyclic monophosphate (100 μM) induced STIM1-YFP translocation to the PM in 11 of 17 β-cells (Fig. 6*E*) and 6 of 10 α-cells (data not shown) identified with epinephrine, and similar effects were seen with another PKA activator (100 μM Sp-8-CPT-cAMPS; data not shown). However, elevation of cAMP with forskolin induced additional PM translocation of STIM1-YFP (Fig. 6*E*, 6 of 8 β-cells). We therefore also tested the effect of 1–2 μM of the Epac activator 8-(4-chlorophenylthio)-2′-*O*-methyladenosine-3′,5′-cyclic monophosphate, acetoxymethyl ester, which also induced STIM1-YFP translocation to the PM in 16 of 26 β-cells (Fig. 6*F*) and 7 of 11 α-cells (data not shown) identified with epinephrine. Our data therefore indicate that both PKA and Epac contribute to mediate the effect of cAMP on STIM1-YFP translocation to the PM.

cAMP-stimulated STIM1 Translocation Does Not Activate SOCE—The effects of cAMP modulation on SOCE were studied using a Ca^{2+} omission-readdition approach in cells that were hyperpolarized with diazoxide and exposed to the Ca^{2+} channel blocker methoxyverapamil to prevent voltage-operated Ca^{2+} entry. The β-cell in Fig. 7*A* was initially exposed to 1.3 mM Ca^{2+} and 3 mM glucose, which causes less than half-maximal Ca^{2+} filling of the ER (19) associated with partial inactivation of the store-operated pathway (21, 25). When subsequent omission of extracellular Ca^{2+} had lowered $[Ca^{2+}]_i$ to a stabile level, the introduction of 10 mM Ca^{2+} induced 18 ± 4 nM

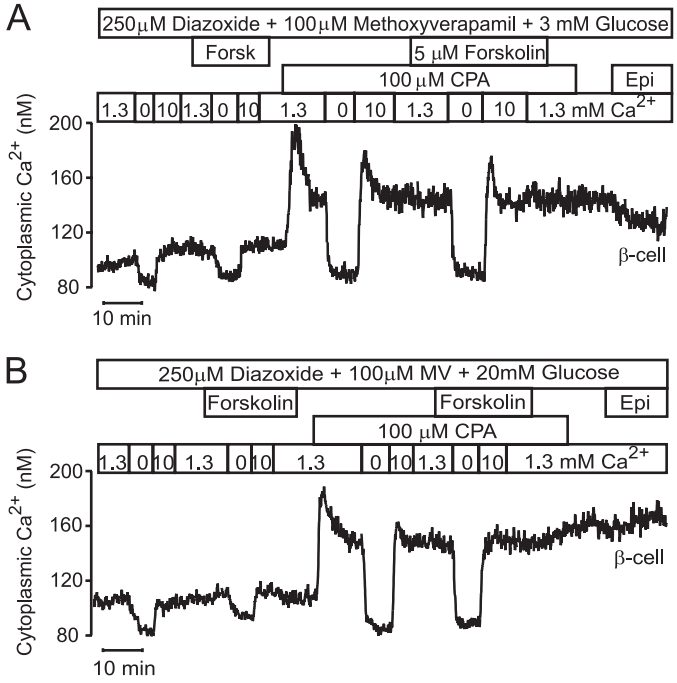

FIGURE 7. **Effects of cAMP elevation on SOCE.** Epifluorescence recordings of $[Ca^{2+}]_i$ in Fura-PE3-loaded large islet cells exposed to 250 μM of the K_{ATP} channel activator diazoxide. Apart from the size, the cells were identified as β-cells based on the lack of response to epinephrine (*Epi*, 5 μM). *A*, forskolin does not affect SOCE in a cell exposed to 3 mM glucose. VOCCs were blocked by hyperpolarization with diazoxide and presence of 100 μM methoxyverapamil. The $[Ca^{2+}]_i$ response to Ca^{2+} omission followed by exposure to 10 mM Ca^{2+} was studied under control conditions and in the presence of 5 μM forskolin before and after full activation of SOCE with 100 μM CPA. *B*, forskolin does not affect SOCE in a cell exposed to 20 mM glucose. Like in *A*, hyperpolarizing diazoxide and the voltage-operated Ca^{2+} channel blocker methoxyverapamil were present throughout. The $[Ca^{2+}]_i$ response to Ca^{2+} omission followed by exposure to 10 mM Ca^{2+} was studied under control conditions and in the presence of 5 μM forskolin before and after full activation of SOCE with 100 μM CPA.

($n = 7$) elevation of $[Ca^{2+}]_i$. The effect of such Ca^{2+} omission-readdition was not altered by forskolin (17 ± 4 nM increase of $[Ca^{2+}]_i$; $n = 7$). When the SOCE was fully activated by emptying the ER with CPA, Ca^{2+} omission-readdition raised $[Ca^{2+}]_i$ by 66 ± 8 nM ($n = 7$; $p < 0.005$). Also under these conditions forskolin failed to affect the response (67 ± 9 nM; $n = 7$).

The effect of cAMP elevation with forskolin on SOCE was also tested in the presence of 20 mM glucose that maximally fills the ER with Ca^{2+} (19) and inhibits the store-operated pathway (21, 25) as well as under conditions when this pathway was activated with CPA (Fig. 7*B*). Again, forskolin had no effect on the Ca^{2+} readdition-induced elevation of $[Ca^{2+}]_i$ under either of these conditions. Before addition of CPA, the increase was 15 ± 5 nM both in the absence and presence of forskolin, and after addition of CPA the increases were 55 ± 4 and 50 ± 4 nM ($n = 6$) in the absence and presence of forskolin, respectively. cAMP-induced accumulation of subplasmalemmal STIM1 apparently occur without effect on SOCE.

cAMP-stimulated STIM1 Translocation Does Not Induce STIM1-Orai1 Co-clustering—Searching for an explanation why cAMP-induced STIM1 translocation did not activate SOCE, we next studied Orai1 distribution in the PM of islet cells expressing Orai1-mCherry alone (data not shown) or in combination with STIM1-YFP (Fig. 8). When the SERCA pump was energized by the presence of 20 mM glucose to fill the ER with calcium and the cells hyperpolarized with diazoxide to prevent triggering of Ca^{2+}-induced Ca^{2+} release, there were few STIM1-YFP puncta at the PM (Fig. 8*A, top panels*). The number of puncta increased markedly in response to forskolin, and the effect was even more striking after depletion of ER Ca^{2+} with CPA. The more pronounced effect of CPA than of forskolin was preferentially observed when STIM1 was co-expressed with Orai-1. In cells expressing STIM1-YFP alone, the total PM-associated STIM1-YFP fluorescence increased 1.64 ± 0.19-fold in the presence of forskolin and 1.82 ± 0.21-fold (not significant, $n = 6$) of control during subsequent exposure to CPA. However, after co-expression with Orai1-mCherry, the total PM-associated STIM1-YFP fluorescence in response to forskolin was 1.31 ± 0.16-fold and that induced by CPA was 2.25 ± 0.24-fold ($p < 0.001$; $n = 8$) of control.

Under control conditions, Orai1-mCherry showed a diffuse distribution with even PM fluorescence and no apparent effect of exposure to forskolin. The variation coefficients in pixel intensities under these conditions were identical (10.2 ± 0.3% for control and 10.3 ± 0.2% for forskolin). However, subsequent SERCA inhibition with CPA induced Orai1-mCherry redistribution with formation of a punctate pattern (Fig. 8*A*, *middle panels*) resulting in a highly significant ($p = 0.001$) increase of the variation coefficient to 13.5 ± 0.4%. The CPA-induced Orai1-mCherry puncta co-localized with those of STIM1-YFP, whereas STIM1-YFP puncta formed in response to forskolin did not associate with increased Orai1-mCherry (Fig. 8*A*, *bottom panels*). To quantify the changes in STIM1 and Orai1, regions of interest (ROIs) were selected corresponding to STIM1 puncta formed either in response to CPA or forskolin, and the STIM1-YFP and Orai1-mCherry fluorescence was then measured in these ROIs. Fig. 8*B* shows that the STIM1-YFP fluorescence within ROIs defined by CPA-induced STIM1-YFP puncta showed a less pronounced increase during exposure to forskolin. However, the Orai1-mCherry fluorescence within these ROIs only increased in response to CPA (Fig. 8*C*). When the ROIs were instead defined by STIM1-YFP puncta formed in response to forskolin, the STIM1-YFP fluorescence within these ROIs also increased after exposure to CPA (Fig. 8*D*). The Orai1-mCherry fluorescence within the same ROIs was not different under basal conditions and in the presence of forskolin but tended to decrease slightly after exposure to CPA (Fig. 8*E*). Orai1 consequently only associates with STIM1 after Ca^{2+} depletion of the ER and preferentially at sites other than those where STIM1 forms puncta in response to forskolin. This conclusion was supported by comparing the location of STIM1 puncta formed in response to forskolin and CPA. As seen in Fig. 8*F,* there was relatively little overlap (*yellow*) between STIM1-YFP puncta formed in response to forskolin (displayed in *red*) and those formed after exposure to CPA (displayed in *green*).

DISCUSSION

This study shows that Ca^{2+} release from the ER and sequestration of the ion in this organelle in the insulin- and glucagon-releasing pancreatic islet cells cause the characteristic translocations of STIM1 to and from the subplasmalemmal junctions,

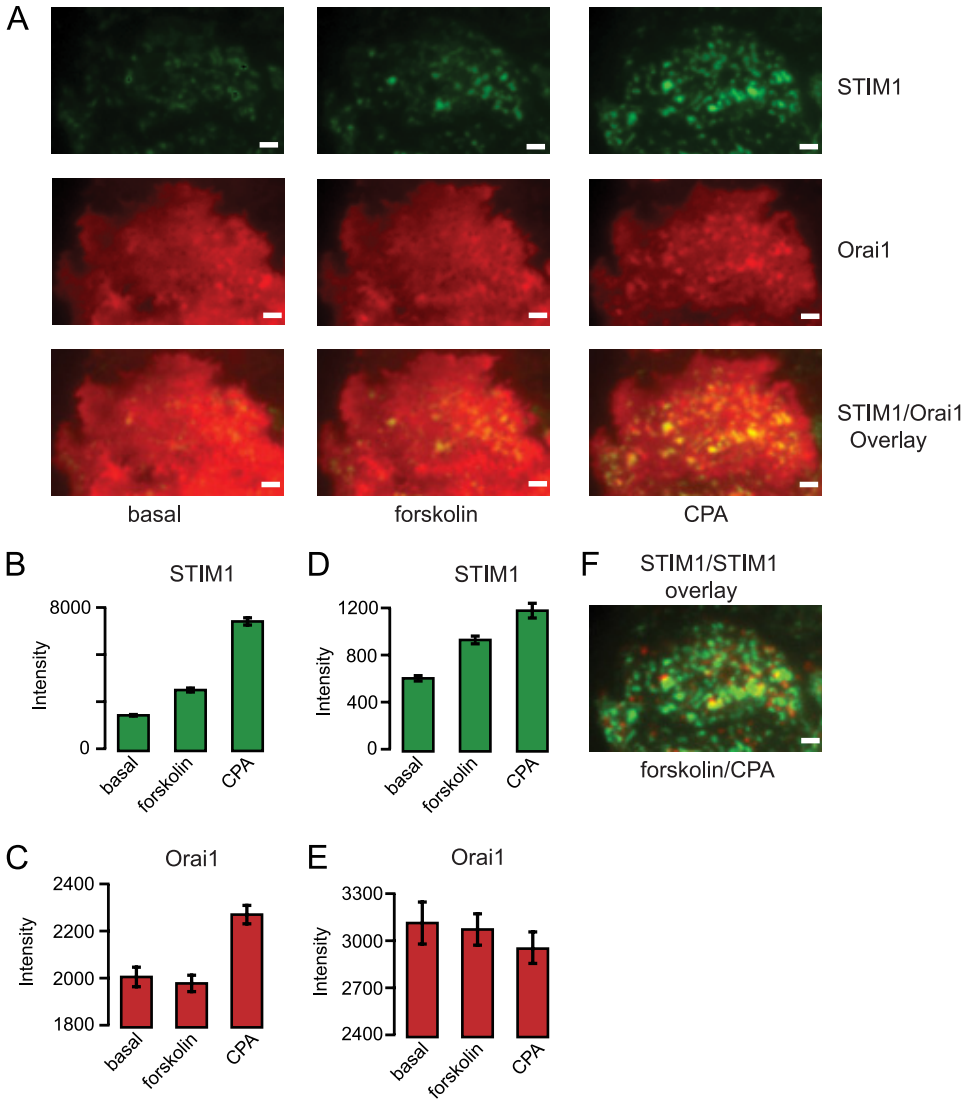

FIGURE 8. **Ca^{2+} store depletion but not cAMP induces STIM1-Orai1 co-clustering in islet cells.** *A*, TIRF images of an islet cell co-expressing STIM1-YFP (*green*) and Orai1-mCherry (*red*). The cell was initially exposed to 20 mM glucose while hyperpolarized with 250 μM of the K_{ATP} channel activator diazoxide (*basal*). Subsequently 5 μM forskolin and 50 μM CPA were added. The *top* and *middle rows* show STIM1 and Orai1 images, respectively, and the *bottom row* shows a STIM1/Orai1 overlay. The images represent averages of 25 consecutive frames under each condition. *B* and *C*, changes in mean STIM1-YFP and Orai1-mCherry fluorescence intensity ± S.E. in 25 ROIs based on selection of STIM1 puncta that were formed after exposure to CPA. *D* and *E*, changes in mean STIM1-YFP and Orai1-mCherry fluorescence intensity ± S.E. in 18 ROIs based on selection of STIM1 puncta that were formed after exposure to forskolin. *F*, overlay image of STIM1 after exposure to forskolin (*red*) and CPA (*green*). Image *scale bars* indicate 1 μm.

respectively. It also demonstrates that epinephrine mimics the effect of Ca^{2+} store depletion in inducing subplasmalemmal accumulation of STIM1 in α-cells but that the opposite effect is observed in β-cells. Searching for the underlying mechanism, we found that cAMP, which increases and decreases in response to epinephrine in α- and β-cells, respectively (34), is involved in the subplasmalemmal accumulation of STIM1. Because the dynamin-related mitochondrial protein mitofusin 2, which was recently implicated in the trafficking of STIM1 to the ER-PM junctions (39), is regulated by PKA (40), we speculate that this mechanism partakes in the cAMP-induced STIM1 translocation. Additional processes are likely involved, as translocation was induced both by specific PKA and Epac agonists. However, although the STIM1 translocation determined by the filling state of the ER affected STIM1-Orai1 co-clustering and modulated SOCE as expected, translocation determined by cAMP occurred without effect on Orai1 and Ca^{2+} entry. Activation of SOCE by Ca^{2+} store depletion has been found to involve a conformational transition that releases the Orai-activating region of STIM1 from an intramolecular clamp (41, 42). Our data indicate that cAMP induces STIM1 translocation independent of such a conformational change.

Glucose is the major physiological stimulator of insulin secretion. The sugar is taken up and metabolized by the β-cells resulting in increased ATP production. An early effect of glucose stimulation is therefore to energize the SERCA pump causing calcium sequestration in the ER, lowering of $[Ca^{2+}]_i$ (20, 43) and initial inhibition of insulin secretion (44, 45). The increased ATP/ADP ratio also closes K_{ATP} channels in the PM with ensuing depolarization. Subsequent opening of L-type VOCCs results in entry of Ca^{2+} and a rise of $[Ca^{2+}]_i$ that trig-

gers a pronounced peak of secretion replacing the initial inhibition (46). ER sequestration of Ca^{2+} is half-maximal and maximal at about 6 and 20 mM glucose, respectively (19, 47–49). It is well documented that Ca^{2+} emptying of the ER activates SOCE in β-cells (19–21, 23, 25, 50), and the rate of SOCE is inversely dependent on the Ca^{2+} filling of the ER in a graded fashion (25). The presently observed glucose-induced STIM1 retranslocation from the PM to the cell interior in mouse β-cells showed somewhat higher glucose sensitivity than Ca^{2+} filling of the ER with half-maximal and maximal effects at 3.4 and 11 mM, respectively. Human β-cells were similar in this respect, but Ca^{2+}-induced Ca^{2+} release may be more prominent in the human cells explaining why peaks of near-membrane STIM1-YFP fluorescence interrupted glucose-induced STIM1 disappearance from the subplasmalemmal region. The physiological relevance of the glucose effects on ER Ca^{2+} filling in β-cells is probably to secure a pool of releasable Ca^{2+} rather than regulating the store-operated pathway, which has modest effects on $[Ca^{2+}]_i$ and insulin secretion (20, 21, 23, 25).

The glucose sensitivity of STIM1 retranslocation to the ER was strikingly higher in α- than in β-cells with maximal effect at 3 mM reinforcing indirect observations that this concentration is sufficient for maximal Ca^{2+} filling of the α-cell ER (22). The different glucose sensitivities cannot be attributed to the fact that α-cells only express SERCA2b, whereas the β-cell also express the lower affinity Ca^{2+} transporter SERCA3 (51). The glucose concentration dependence of ER Ca^{2+} filling in β-cells is thus unaffected after SERCA3 knock-out (52). SOCE in α-cells is consequently controlled by the same low glucose concentrations that regulate glucagon release. Because α-cells have a higher input resistance than β-cells, the membrane potential is sensitive to small changes in current (53). Therefore, SOCE has a much more pronounced effect in α-cells, depolarizing the membrane sufficiently to trigger Ca^{2+} influx through VOCCs (22) and glucagon release (24). Epinephrine stimulates glucagon secretion in this manner by binding to α_1- and β-adrenoceptors (32) leading to ER release of Ca^{2+} with resulting SOCE and VOCC activation (22). We have proposed that glucose also modulates glucagon secretion via the store-operated mechanism. Under normoglycemic conditions the ER is filled with Ca^{2+}, and there is no SOCE activation and thus no depolarization to activate the VOCCs. By contrast, when glucose declines to hypoglycemic levels, the ER begins to empty, and the resulting SOCE activation provides the membrane depolarization that triggers VOCC activation and glucagon release (22, 24).

In summary, this study shows that STIM1 accumulates in the subplasmalemmal region in response to Ca^{2+} depletion of the ER in α- and β-cells and that glucose-induced Ca^{2+} refilling of the ER stimulates the opposite translocation. The observation that a glucose concentration as low as 3 mM causes maximal retranslocation of STIM1 to the ER in α-cells is consistent with the idea that the sugar inhibits glucagon secretion by shutting off the store-operated pathway. We also found that cAMP stimulates subplasmalemmal accumulation of STIM1 in both α- and β-cells. However, the cAMP-induced STIM1 puncta formed without co-clustering of Orai1 or activation of SOCE. Apparently, factors in addition to STIM1 translocation are required for the formation of functional Orai1 channels and activation of SOCE.

Acknowledgments—We are indebted to Heléne Dansk and Ing-Marie Mörsare for technical assistance and to Professor Sir Michael Berridge, Babraham Institute, Cambridge, United Kingdom, for critically reading the manuscript. Human pancreatic islets were obtained from The Nordic Network for Clinical Islet Transplantation, supported by the Swedish National Strategic Research Initiative Exodiab (Excellence of Diabetes Research in Sweden) and the Juvenile Diabetes Research Foundation.

REFERENCES

1. Putney, J. W., Jr. (1986) A model for receptor-regulated calcium entry. *Cell Calcium* **7,** 1–12
2. Roos, J., DiGregorio, P. J., Yeromin, A. V., Ohlsen, K., Lioudyno, M., Zhang, S., Safrina, O., Kozak, J. A., Wagner, S. L., Cahalan, M. D., Veliçelebi, G., and Stauderman, K. A. (2005) STIM1, an essential and conserved component of store-operated Ca^{2+} channel function. *J. Cell Biol.* **169,** 435–445
3. Liou, J., Kim, M. L., Heo, W. D., Jones, J. T., Myers, J. W., Ferrell, J. E., Jr., and Meyer, T. (2005) STIM is a Ca^{2+} sensor essential for Ca^{2+} store-depletion-triggered Ca^{2+} influx. *Curr. Biol.* **15,** 1235–1241
4. Spassova, M. A., Soboloff, J., He, L. P., Xu, W., Dziadek, M. A., and Gill, D. L. (2006) STIM1 has a plasma membrane role in the activation of store-operated Ca^{2+} channels. *Proc. Natl. Acad. Sci. U.S.A.* **103,** 4040–4045
5. Lewis, R. S. (2007) The molecular choreography of a store-operated calcium channel. *Nature* **446,** 284–287
6. Cahalan, M. D., Zhang, S. L., Yeromin, A. V., Ohlsen, K., Roos, J., and Stauderman, K. A. (2007) Molecular basis of the CRAC channel. *Cell Calcium* **42,** 133–144
7. Vig, M., Peinelt, C., Beck, A., Koomoa, D. L., Rabah, D., Koblan-Huberson, M., Kraft, S., Turner, H., Fleig, A., Penner, R., and Kinet, J. P. (2006) CRACM1 is a plasma membrane protein essential for store-operated Ca^{2+} entry. *Science* **312,** 1220–1223
8. Feske, S., Gwack, Y., Prakriya, M., Srikanth, S., Puppel, S. H., Tanasa, B., Hogan, P. G., Lewis, R. S., Daly, M., and Rao, A. (2006) A mutation in Orai1 causes immune deficiency by abrogating CRAC channel function. *Nature* **441,** 179–185
9. Zhang, S. L., Yeromin, A. V., Zhang, X. H., Yu, Y., Safrina, O., Penna, A., Roos, J., Stauderman, K. A., and Cahalan, M. D. (2006) Genome-wide RNAi screen of Ca^{2+} influx identifies genes that regulate Ca^{2+} release-activated Ca^{2+} channel activity. *Proc. Natl. Acad. Sci. U.S.A.* **103,** 9357–9362
10. Peinelt, C., Vig, M., Koomoa, D. L., Beck, A., Nadler, M. J., Koblan-Huberson, M., Lis, A., Fleig, A., Penner, R., and Kinet, J. P. (2006) Amplification of CRAC current by STIM1 and CRACM1 (Orai1). *Nat. Cell Biol.* **8,** 771–773
11. Soboloff, J., Spassova, M. A., Tang, X. D., Hewavitharana, T., Xu, W., and Gill, D. L. (2006) Orai1 and STIM reconstitute store-operated calcium channel function. *J. Biol. Chem.* **281,** 20661–20665
12. Mercer, J. C., Dehaven, W. I., Smyth, J. T., Wedel, B., Boyles, R. R., Bird, G. S., and Putney, J. W., Jr. (2006) Large store-operated calcium selective currents due to co-expression of Orai1 or Orai2 with the intracellular calcium sensor, Stim1. *J. Biol. Chem.* **281,** 24979–24990
13. Prakriya, M., Feske, S., Gwack, Y., Srikanth, S., Rao, A., and Hogan, P. G. (2006) Orai1 is an essential pore subunit of the CRAC channel. *Nature* **443,** 230–233
14. Yeromin, A. V., Zhang, S. L., Jiang, W., Yu, Y., Safrina, O., and Cahalan, M. D. (2006) Molecular identification of the CRAC channel by altered ion selectivity in a mutant of Orai. *Nature* **443,** 226–229
15. Zhang, S. L., Yu, Y., Roos, J., Kozak, J. A., Deerinck, T. J., Ellisman, M. H., Stauderman, K. A., and Cahalan, M. D. (2005) STIM1 is a Ca^{2+} sensor that activates CRAC channels and migrates from the Ca^{2+} store to the plasma

membrane. *Nature* **437,** 902–905
16. Chvanov, M., Walsh, C. M., Haynes, L. P., Voronina, S. G., Lur, G., Gerasimenko, O. V., Barraclough, R., Rudland, P. S., Petersen, O. H., Burgoyne, R. D., and Tepikin, A. V. (2008) ATP depletion induces translocation of STIM1 to puncta and formation of STIM1-ORAI1 clusters. Translocation and retranslocation of STIM1 does not require ATP. *Pflugers Arch.* **457,** 505–517
17. Putney, J. W., Jr. (2007) New molecular players in capacitative Ca^{2+} entry. *J. Cell Sci.* **120,** 1959–1965
18. Putney, J. W. (2009) Capacitative calcium entry. From concept to molecules. *Immunol. Rev.* **231,** 10–22
19. Gylfe, E. (1991) Carbachol induces sustained glucose-dependent oscillations of cytoplasmic Ca^{2+} in hyperpolarized pancreatic β cells. *Pflugers Arch.* **419,** 639–643
20. Chow, R. H., Lund, P. E., Löser, S., Panten, U., and Gylfe, E. (1995) Coincidence of early glucose-induced depolarization with lowering of cytoplasmic Ca^{2+} in mouse pancreatic β-cells. *J. Physiol.* **485,** 607–617
21. Liu, Y. J., and Gylfe, E. (1997) Store-operated Ca^{2+} entry in insulin-releasing pancreatic β-cells. *Cell Calcium* **22,** 277–286
22. Liu, Y. J., Vieira, E., and Gylfe, E. (2004) A store-operated mechanism determines the activity of the electrically excitable glucagon-secreting pancreatic α-cell. *Cell Calcium* **35,** 357–365
23. Worley, J. F., 3rd, McIntyre, M. S., Spencer, B., Mertz, R. J., Roe, M. W., and Dukes, I. D. (1994) Endoplasmic reticulum calcium store regulates membrane potential in mouse islet β-cells. *J. Biol. Chem.* **269,** 14359–14362
24. Vieira, E., Salehi, A., and Gylfe, E. (2007) Glucose inhibits glucagon secretion by a direct effect on mouse pancreatic α-cells. *Diabetologia* **50,** 370–379
25. Dyachok, O., and Gylfe, E. (2001) Store-operated influx of Ca^{2+} in pancreatic β-cells exhibits graded dependence on the filling of the endoplasmic reticulum. *J. Cell Sci.* **114,** 2179–2186
26. Tamarina, N. A., Kuznetsov, A., and Philipson, L. H. (2008) Reversible translocation of EYFP-tagged STIM1 is coupled to calcium influx in insulin secreting β-cells. *Cell Calcium* **44,** 533–544
27. Goto, M., Eich, T. M., Felldin, M., Foss, A., Källen, R., Salmela, K., Tibell, A., Tufveson, G., Fujimori, K., Engkvist, M., and Korsgren, O. (2004) Refinement of the automated method for human islet isolation and presentation of a closed system for *in vitro* islet culture. *Transplantation* **78,** 1367–1375
28. Dyachok, O., Idevall-Hagren, O., Sågetorp, J., Tian, G., Wuttke, A., Arrieumerlou, C., Akusjärvi, G., Gylfe, E., and Tengholm, A. (2008) Glucose-induced cyclic AMP oscillations regulate pulsatile insulin secretion. *Cell Metab.* **8,** 26–37
29. Lernmark, Å. (1974) The preparation of, and studies on, free cell suspensions from mouse pancreatic islets. *Diabetologia* **10,** 431–438
30. Grynkiewicz, G., Poenie, M., and Tsien, R. Y. (1985) A new generation of Ca^{2+} indicators with greatly improved fluorescence properties. *J. Biol. Chem.* **260,** 3440–3450
31. Koh, G., Seino, Y., Tsuda, K., Nishi, S., Ishida, H., Takeda, J., Fukumoto, H., Taminato, T., and Imura, H. (1987) Effect of the α2-blocker DG-5128 on insulin and somatostatin release from the isolated perfused rat pancreas. *Life Sci.* **40,** 1113–1118
32. Vieira, E., Liu, Y. J., and Gylfe, E. (2004) Involvement of α1- and β-adrenoceptors in adrenaline stimulation of the glucagon-secreting mouse α-cell. *Naunyn Schmiedebergs Arch. Pharmacol.* **369,** 179–183
33. Schuit, F. C., and Pipeleers, D. G. (1986) Differences in adrenergic recognition by pancreatic A and B cells. *Science* **232,** 875–877
34. Tian, G., Sandler, S., Gylfe, E., and Tengholm, A. (2011) Glucose- and hormone-induced cAMP oscillations in α- and β-cells within intact pancreatic islets. *Diabetes* **60,** 1535–1543
35. Nakaki, T., Nakadate, T., and Kato, R. (1980) α2-Adrenoceptors modulating insulin release from isolated pancreatic islets. *Naunyn Schmiedebergs Arch. Pharmacol.* **313,** 151–153
36. Liu, Y. J., Grapengiesser, E., Gylfe, E., and Hellman, B. (1996) Cross-talk between the cAMP and inositol trisphosphate-signaling pathways in pancreatic β-cells. *Arch. Biochem. Biophys.* **334,** 295–302
37. Dzhura, I., Chepurny, O. G., Leech, C. A., Roe, M. W., Dzhura, E., Xu, X., Lu, Y., Schwede, F., Genieser, H. G., Smrcka, A. V., and Holz, G. G. (2011) Phospholipase C-ε links Epac2 activation to the potentiation of glucose-stimulated insulin secretion from mouse islets of Langerhans. *Islets* **3,** 121–128
38. Shen, W. W., Frieden, M., and Demaurex, N. (2011) Local cytosolic Ca^{2+} elevations are required for stromal interaction molecule 1 (STIM1) de-oligomerization and termination of store-operated Ca^{2+} entry. *J. Biol. Chem.* **286,** 36448–36459
39. Singaravelu, K., Nelson, C., Bakowski, D., de Brito, O. M., Ng, S. W., Di Capite, J., Powell, T., Scorrano, L., and Parekh, A. B. (2011) Mitofusin 2 regulates STIM1 migration from the Ca^{2+} store to the plasma membrane in cells with depolarized mitochondria. *J. Biol. Chem.* **286,** 12189–12201
40. Zhou, W., Chen, K. H., Cao, W., Zeng, J., Liao, H., Zhao, L., and Guo, X. (2010) Mutation of the protein kinase A phosphorylation site influences the anti-proliferative activity of mitofusin 2. *Atherosclerosis* **211,** 216–223
41. Korzeniowski, M. K., Manjarrés, I. M., Varnai, P., and Balla, T. (2010) Activation of STIM1-Orai1 involves an intramolecular switching mechanism. *Sci. Signal.* **3,** ra82
42. Muik, M., Fahrner, M., Schindl, R., Stathopulos, P., Frischauf, I., Derler, I., Plenk, P., Lackner, B., Groschner, K., Ikura, M., and Romanin, C. (2011) STIM1 couples to ORAI1 via an intramolecular transition into an extended conformation. *EMBO J.* **30,** 1678–1689
43. Gylfe, E. (1988) Glucose-induced early changes in cytoplasmic calcium of pancreatic β-cells studied with time-sharing dual-wavelength fluorometry. *J. Biol. Chem.* **263,** 5044–5048
44. Hellman, B., Hällgren, R., Abrahamsson, H., Bergsten, P., Berne, C., Gylfe, E., Rorsman, P., and Wide, L. (1985) The dual action of glucose on the cytosolic Ca^{2+} activity in pancreatic β-cells. Demonstration of an inhibitory effect of glucose on insulin release in the mouse and man. *Biomed. Biochim. Acta* **44,** 63–70
45. Hellman, B., Gylfe, E., Grapengiesser, E., Lund, P. E., and Marcström, A. (1992) in *Nutrient Regulation of Insulin Secretion* (Flatt, P. R., ed.) pp 213–246, Portland Press Ltd., Colchester, UK
46. Ashcroft, F. M., and Rorsman, P. (1989) Electrophysiology of the pancreatic β-cell. *Prog. Biophys. Mol. Biol.* **54,** 87–143
47. Gylfe, E. (1988) Nutrient secretagogues induce bimodal early changes in cytoplasmic calcium of insulin-releasing ob/ob mouse β-cells. *J. Biol. Chem.* **263,** 13750–13754
48. Tengholm, A., Hellman, B., and Gylfe, E. (1999) Glucose regulation of free Ca^{2+} in the endoplasmic reticulum of mouse pancreatic beta cells. *J. Biol. Chem.* **274,** 36883–36890
49. Tengholm, A., Hellman, B., and Gylfe, E. (2001) The endoplasmic reticulum is a glucose-modulated high affinity sink for Ca^{2+} in mouse pancreatic β-cells. *J. Physiol.* **530,** 533–540
50. Thore, S., Dyachok, O., Gylfe, E., and Tengholm, A. (2005) Feedback activation of phospholipase C via intracellular mobilization and store-operated influx of Ca^{2+} in insulin-secreting β-cells. *J. Cell Sci.* **118,** 4463–4471
51. Arredouani, A., Guiot, Y., Jonas, J. C., Liu, L. H., Nenquin, M., Pertusa, J. A., Rahier, J., Rolland, J. F., Shull, G. E., Stevens, M., Wuytack, F., Henquin, J. C., and Gilon, P. (2002) SERCA3 ablation does not impair insulin secretion but suggests distinct roles of different sarcoendoplasmic reticulum Ca^{2+} pumps for Ca^{2+} homeostasis in pancreatic β-cells. *Diabetes* **51,** 3245–3253
52. Ravier, M. A., Daro, D., Roma, L. P., Jonas, J. C., Cheng-Xue, R., Schuit, F. C., and Gilon, P. (2011) Mechanisms of control of the free Ca^{2+} concentration in the endoplasmic reticulum of mouse pancreatic β-cells. Interplay with cell metabolism and $[Ca^{2+}]_c$ and role of SERCA2b and SERCA3. *Diabetes* **60,** 2533–2545
53. Barg, S., Galvanovskis, J., Göpel, S. O., Rorsman, P., and Eliasson, L. (2000) Tight coupling between electrical activity and exocytosis in mouse glucagon-secreting α-cells. *Diabetes* **49,** 1500–1510